



Egyptian Society of Radiology and Nuclear Medicine
The Egyptian Journal of Radiology and Nuclear Medicine

www.elsevier.com/locate/ejrnrm
www.sciencedirect.com



ORIGINAL ARTICLE

Using morphological transforms to enhance the contrast of medical images



Hamid Hassanpour¹, Najmeh Samadiani^{*,1}, S.M. Mahdi Salehi¹

Department of Computer Engineering and Information Technology, University of Shahrood, Shahrood, Iran

Received 16 September 2014; accepted 13 January 2015

Available online 7 February 2015

KEYWORDS

Mathematical morphology;
Top-Hat transforms;
Contrast Improvement Ratio
(CIR);
Enhancement of medical
images;
Gamma correction

Abstract Medical imaging plays an important role in monitoring the patient's health condition and providing an effective treatment. However, the existence of several objects overlapping in an image and the close proximity of adjacent pixels values in medical images make the diagnostic process a difficult task. To cope with such problems, this paper presents a new method based on morphological transforms to enhance the quality of various medical images. In this method, a disk-shaped mask whose size fits that of the original input image is chosen for morphological operations. Afterward, the proposed filter from the Top-Hat transforms is applied to the image, using the chosen mask in a multi-step process. At each step, the size of the mask is increased. Consequently, an enhanced image is provided for each mask size. The number of required steps and the final enhanced image are determined based on the Contrast Improvement Ratio (CIR) measure. Indeed, this approach applies an exfoliation process on the images, in which one or several objects in the image are prominently manifested using morphological filter, hence provide an appropriate image for analysis. The results in this research indicate that the proposed approach makes a better contrast and works much better than the other existing methods in improving the quality of medical images.

© 2015 The Authors. The Egyptian Society of Radiology and Nuclear Medicine. Production and hosting by Elsevier B.V. This is an open access article under the CC BY-NC-ND license (<http://creativecommons.org/licenses/by-nc-nd/4.0/>).

1. Introduction

Medical images have an important role in diagnosing a disease and monitoring the effect of the selected treatments. In spite of the increasing progress in the methods of capturing these images, the produced images may not pose enough quality for an accurate diagnosis. Emergency situations, environmental

noises, patients' special conditions in photography, lighting conditions and technical constraints of imaging devices are among the reasons why images may have low quality (1–3). In such cases, image enhancement techniques can be useful, especially when reimaging is impossible. These new techniques are used to repair the damaged images and to enhance their quality and contrast.

The method presented in (1) enhances a medical image using wavelet transformation. In this method, the high-frequency sub-images are decomposed using the Haar wavelet transform. Then, noise in the high-frequency sub-bands is reduced using soft-thresholding. Finally, the enhanced image is obtained using inverse wavelet transformation. Another

* Corresponding author. Tel.: +98 9151871285.

E-mail address: najmeh_sam@yahoo.com (N. Samadiani).

¹ Tel.: +98 2332300251.

Peer review under responsibility of Egyptian Society of Radiology and Nuclear Medicine.

<http://dx.doi.org/10.1016/j.ejrnrm.2015.01.004>

0378-603X © 2015 The Authors. The Egyptian Society of Radiology and Nuclear Medicine. Production and hosting by Elsevier B.V. This is an open access article under the CC BY-NC-ND license (<http://creativecommons.org/licenses/by-nc-nd/4.0/>).

method was presented for enhancing CT medical images based on Gaussian Scale Mixture (GSM) model for wavelet coefficients in multi-scale wavelet analysis in (4). In this method, first, noise is removed from the noisy image using Wiener filter. Then, through the qualitative analysis and classification of wavelet coefficients for the signal and noise, the wavelet's approximate distribution and statistical characteristics are described, combining GSM model for wavelet coefficient. This algorithm can enhance CT images whose noise is removed.

Another common method for medical image enhancement is histogram equalization (5) that enhances the contrast of image by increasing distribution of gray levels. This method does not necessarily obtain good results for all areas of an image because contrast enhancement may damage the image and the border areas. Because of this, there are different generalizations of this method to improve its performance (6,7). An algorithm for improving abdominal ultrasound images is proposed based on combination of histogram equalization and wavelet transformation in (8). This algorithm improves edges and surroundings of abdominal walls and has real time performance in dynamic applications.

Another method for medical image enhancement is Gamma correction (9). In this method, Gamma values of individual pixels are locally optimized by minimizing the homogeneity of co-occurrence matrix of the original image. The Gamma correction method enhances dynamic range and improves the image.

In (10) a morphological filter is proposed for sharpening medical images. In this method, after locating edges by gradient-based operators, a class of morphological filter is applied to sharpen the existing edges. In fact, morphology operators, through increasing and decreasing colors in different parts of an image, have an important role in processing and detecting various existing objects in the image. Locating edges in an image using morphology gradient is an example that has comparable performance with that of classic edge-detectors such as Canny and Sobel (11). In another method presented in (12), vessels in angiography images are enhanced based on their special patterns and morphological filters.

In capturing a medical image from body, since different organs are in various depths, the image does not have sound quality to be analyzed by the physician. For instance, in an image taken from chest by X-ray or ultrasound, organs such as skin, heart, lung, bone, ligaments, vessels, cartilage and lymphatic fluid appear simultaneously in an image while overlapping. Since each body organ has different structure or texture, we can prominent one or several of them in the image using morphological filter, hence provide an appropriate image for analysis. We name this as an exfoliation process. A similar function is performed in processing aerial images (taken by airplane or balloon) to remove clouds to achieve more clarity (13).

In the present study, a new method based on particular transforms of mathematical morphology is proposed to enhance the contrast of medical images. To do so, we first determine the shape and size of the desired mask for morphological transforms. Achieving suitable result and reducing computation time in morphology-based methods depend on the shape and size of a mask; so, the selected mask for a problem should be in appropriate shape and size. Generally, the desired mask is selected arbitrarily. Since disk-shaped mask is independent of changes in rotation, it is more commonly used in medical imaging compared to type of masks. The size

of mask is also dependent on input image and can take different values for different images; therefore, in the proposed method, we use a disk-shaped mask to apply morphology transforms whose initial size is determined through trial and error and based on the input image. Then, exfoliation process is done by applying a filter of Top-Hat transforms using different masks in various radii. We will have an enhanced image per each mask. The best enhanced image is selected among the produced images using Contrast Improvement Ratio (CIR).

The organization of the paper is as follows: Section 2 introduces the images under study. Section 3 explains general mechanisms of mathematical morphology method such as operators, selecting proper mask and Top-Hat transforms and CIR. In Section 4, the proposed algorithm is described. The result of applying the proposed method and its comparison with other improvement methods is analyzed in Section 5 and conclusion will be the last section.

2. The medical images under study

The medical images used in this paper are CT-Scan and X-ray images. The CT-Scan images have been taken from different parts of body such as chest, abdomen and brain which are used by a physician to determine skeletal problems, size and location of a tumor and diseases of blood vessels; and give guidelines for surgical processes and chemotherapy treatments for cancer. The X-ray images were taken from foot, hand and chest. These images can also be enhanced using the proposed method. The CT-Scan and radiology images used in this paper are in resolution of 72 pixel/in.

3. Mathematical morphology

Methods of mathematical morphology act based on the structural properties of objects. These methods use mathematical principles and relationships between categories to extract the components of an image, which are useful in describing the shape of zones. Morphological operators are nonlinear, and two sets of data are their input. The first set contains the original image and the second one describes the structural element (mask). The original image is binary or in gray level and the mask is a matrix containing zero and one values (12).

It is after applying the final image to the morphological operators that a new value for each pixel is obtained through sliding the mask on the original image. Value 1 in each mask indicates effectiveness and value 0 indicates ineffectiveness in the final image. Different formats can be selected to form a mask. Fig. 1 shows a disk-shaped mask with radius of 4 (9 * 9 matrix).

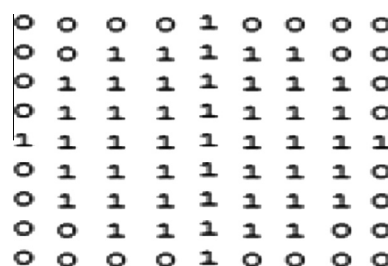


Fig. 1 Disk-shaped structural element (mask) with radius of 4.

3.1. morphological operators

If $A(x, y)$ and $B(u, v)$ describe the gray-level image matrix and the structural element matrix respectively, erosion and dilation operators are defined as (1) and (2):

$$A \ominus B = \min_{u,v} \{A(x+u, y+v) - B(u, v)\} \quad (1)$$

$$A \oplus B = \max_{u,v} \{A(x-u, y-v) + B(u, v)\} \quad (2)$$

The erosion operator reduces the size of objects. This operator increases the size of holes in an image and removes very small details of that image. Removing bright areas under the mask makes the final image looks darker than the original image. The dilation operator acts in reverse; in other words, it increases and decreases the size of objects and holes in the image respectively. The opening operator is equivalent to the application of the erosion and dilation operations on the same image respectively (Eq. (3)) while the closing operator acts in reverse (Eq. (4)):

$$A \circ B = (A \ominus B) \oplus B \quad (3)$$

$$A \cdot B = (A \oplus B) \ominus B \quad (4)$$

The opening operator removes weak connections between objects and small details while the closing operator removes small holes and fills cracks.

3.2. Selecting a proper mask

Selecting a mask in proper shape and size to take morphological actions has a key role in achieving desired results and reducing calculation time. In general, the shape and size of a mask are arbitrarily selected; however, the selected mask should be in appropriate shape and size for various diagnosis purposes. Disk-shaped masks (Fig. 1) are more commonly used for medical images than other masks. As stated before, since disk-shaped masks are independent of changes in rotation, they are chosen for medical images.

Since big or small masks strengthen or weaken various parts of an image, it is impossible to gather detailed information on the contrast of different images using only one structural element. This is why one mask in a particular shape and size may not appropriate for other applications (14).

In the proposed method, the change in shape and size of the mask continues until an appropriate result obtained. It should be mentioned that past experiences have key roles in selecting proper masks to take morphological actions.

3.3. Top-Hat transforms

These transforms are used to enhance the contrast of images through morphological methods and are in two general types: Top-Hat transform is obtained by subtracting the opening of the original image from the image itself (Eq. (5)), and Bottom-Hat transform is obtained through subtracting the original image from its closing (Eq. (6)) (15):

$$\text{Top-Hat}(A) = A_{TH} = A - (A \circ B) \quad (5)$$

$$\text{Bottom-Hat}(A) = A_{BH} = (A \cdot B) - A \quad (6)$$

Top-Hat and Bottom-Hat transforms are generally known as Open Top-Hat or White Top-Hat and Close Top-Hat or Black Top-Hat respectively. In many papers, Top-Hat is used to refer to both kinds of hat transforms. These transforms are named Top-Hat after Cylinder Hat shown in Fig. 2. Fig. 2(a) shows an image of the cross-section of the transform and Fig. 2(b) describes defined parameters. In this figure, h indicates the difference in contrast and acts as a threshold, and d_0 and d_i determine radius of the circles (16).

According to Eq. (5), since the opening operator leaves a background of the image, it is expected that Top-Hat transform removes the image background. This transform acts like a high-pass filter and extracts the bright areas of the image (with contrast not less than h) which are smaller than the mask. Bottom-Hat transform also removes the background of the image and leaves some dark areas of the image which are smaller than the mask itself (17).

It is possible to add the bright areas (the results of the opening operator) to the image and subtract the dark areas (the results of the closing operator) from it. As a result, there will be an enhancement in the contrast between bright and dark areas:

$$A_o = A + A_{TH} - A_{BH} \quad (7)$$

Fig. 3(b) and (c) shows the results of applying Top-Hat and Bottom-Hat transforms for a CT-Scan image. Fig. 3(d) shows the result of applying (7) (disk with radius 7) to the image. In comparison with the original image, this final image is highly enhanced. Fig. 3(e) has been obtained similarly, but using a disk with radius 37. That is why this image has a better quality.

3.4. Contrast improvement ratio

Contrast which is defined as the difference in visual properties of pixels makes an object distinguishable from other objects and the background. In gray-scale images, contrast is determined by the difference in the brightness of the object and its surroundings. In this paper, we use CIR to measure contrast. CIR measures the effect of contrast enhancement on image quality (18). In this method, we compute the mean value of luminance in two different concentric rectangular windows centered on each pixel. More specifically, we can define the local contrast as the following ratio:

$$c(x, y) = \frac{|p - a|}{|p + a|} \quad (8)$$

where p and a are the average values of gray levels in the center window and the surrounding window of the pixel location

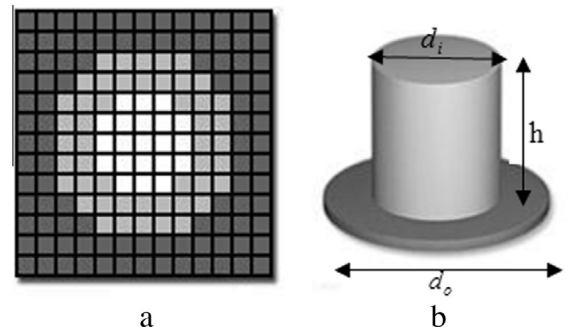


Fig. 2 General idea in Top-Hat transform, (a) cross-section of the transform, (b) parameters of the transform.

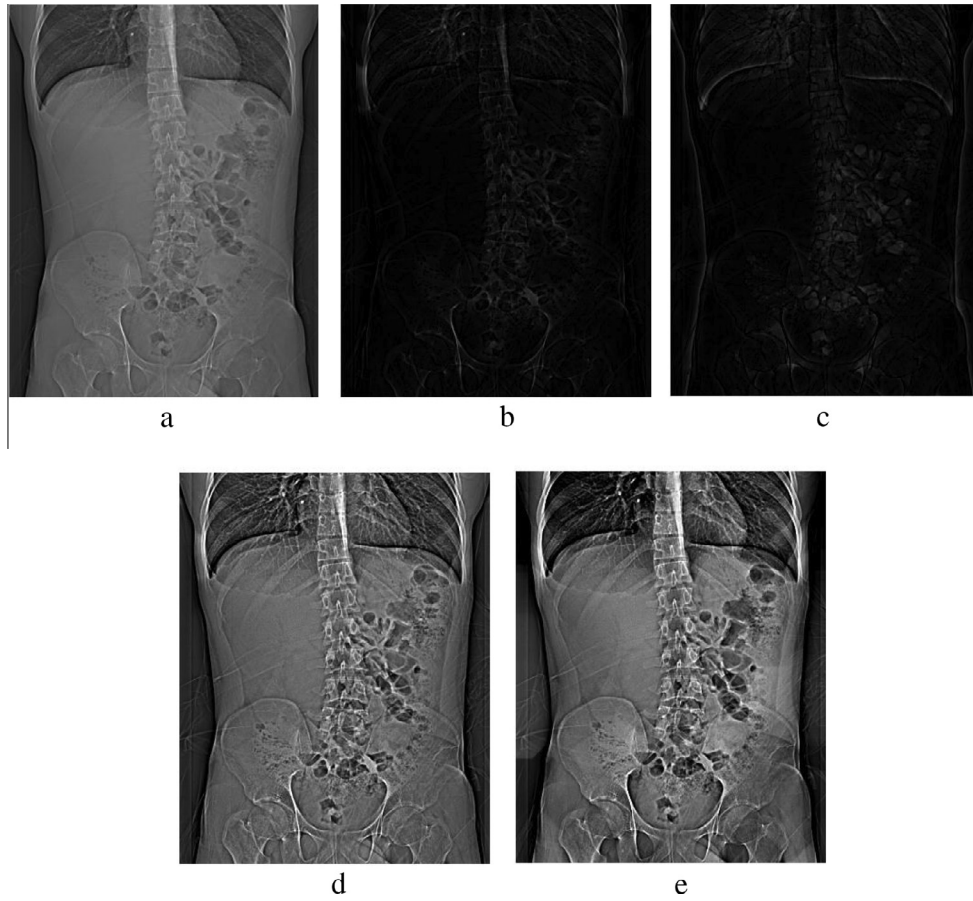


Fig. 3 The results of morphological operators in the improvement of a CT-Scan image. A disk with radius 7 has been used for the structural elements (b) to (d). (a) Original image, (b) Top-Hat transform, (c) Bottom-Hat transform, (d) using Eq. (7), (e) using Eq. (7) for disk with radius 37.

(x, y) respectively. The inner window is a 3×3 and the outer one is a 7×7 square. Here $c(x, y)$ is the contrast measurement and is in the range of $[0, 1]$. Finally, CIR is defined as the following ratio using the enhanced and original image local contrast measurements.

$$\text{CIR} = \frac{\sum_{(x,y) \in R} (c(x, y) - \hat{c}(x, y))^2}{\sum_{(x,y) \in R} c^2(x, y)} \quad (9)$$

where R is the region of interest and c and \hat{c} are the local contrast measurements in original and enhanced images respectively (19).

4. Proposed method

According to 3–2, this paper aimed at using a mask and increasing its size exponentially to obtain an image with appropriate contrast. To do so, we repeat the dilation operation on the initial mask to gradually increase its size and analyze the result in each stage. In this method, mask B_i is obtained by carrying out the dilation operation on mask B , i times; it is obvious that $B_1 = B$.

$$B_i = B \oplus B \oplus \dots \oplus B \quad (10)$$

This procedure continues to achieve the desired image. So, Eqs. (5) and (6) are generalized:

$$A_{TH_i} = A - (A \circ B_i) \quad (11)$$

$$A_{BH_i} = (A \cdot B_i) - A \quad (12)$$

Leading to the generalization of Eq. (7):

$$A_o = A + A_{TH_i} - A_{BH_i} \quad (13)$$

Therefore, we propose a method which can produce several contrasts on the image by measuring the discrepancy between the results of the Top-Hat and Bottom-Hat transforms to select the optimized contrast. The general stages are as follows:

- i. Taking the input image and determining the shape and size of the mask

In the first stage, we use a disk-shaped mask with the initial radius 30. The size of the radius is increased arbitrarily according to the size of the original image in the following stages.

- ii. Using Top-Hat transforms

We use Eq. (14) to produce the final image. i and m parameters control the size of the mask and the produced contrast respectively. The value of i is selected from among whole numbers while it is possible to select the value of m from decimal numbers. In a particular case, $m = i = 1$, we obtain Eq. (7).

$$A_o = A + m(A_{TH_i} - A_{BH_i}) \quad (14)$$

iii. Selecting the final image by CIR

For i different selecting from masks and m selecting from control coefficients, we will have $m*i$ produced images in output which we automatically choose the most proper of them

using CIR. As stated before, when the proposed filter of morphological transform is applied to the masks with various radii in an increasing manner, we will have an enhanced image per mask. We should select the best enhanced image. In each step, the contrast improvement is measured by CIR through

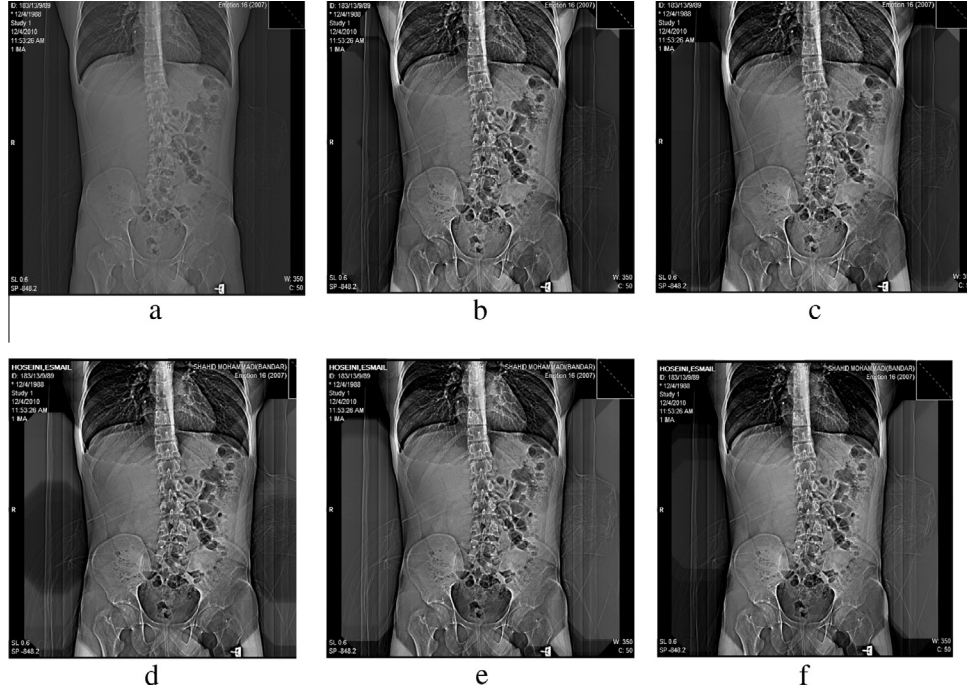


Fig. 4 (a) Original image, (b) the first enhanced image with the disk in size 30 and CIR = 0.1202, (c) the second enhanced image with the disk in size 40 and CIR = 0.1360, (d) the third enhanced image with the disk in size 50 and CIR = 0.1899, (e) the final enhanced image with the disk in size 60 and CIR = 0.3573, (f) the enhanced image with the disk in size 70 and CIR = 0.3179, since image (e) has less values than the previous image, it is selected as the final image.

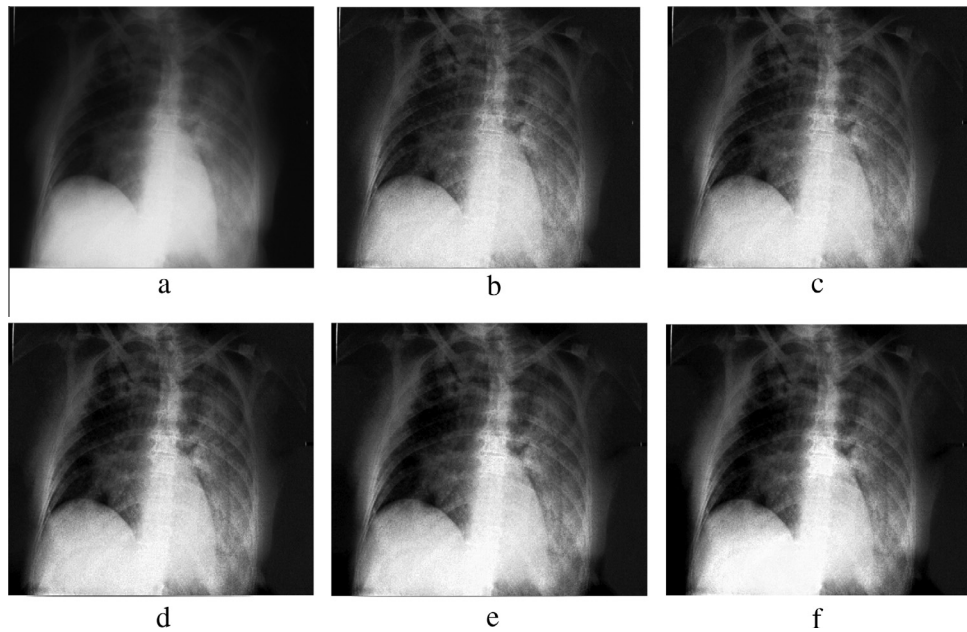


Fig. 5 (a) The original image, (b) the first enhanced image with the disk in size 30 and CIR = 0.0754, (c) the second enhanced image with the disk in size 40 and CIR = 0.2256, (d) the third enhanced image with the disk in size 50 and CIR = 0.6868, (e) the final enhanced image with the disk in size 60 and CIR = 0.7647, (f) the enhanced image with the disk in size 70 and CIR = 0.6694, since image (e) has less values than the previous image, it is selected as the final image.

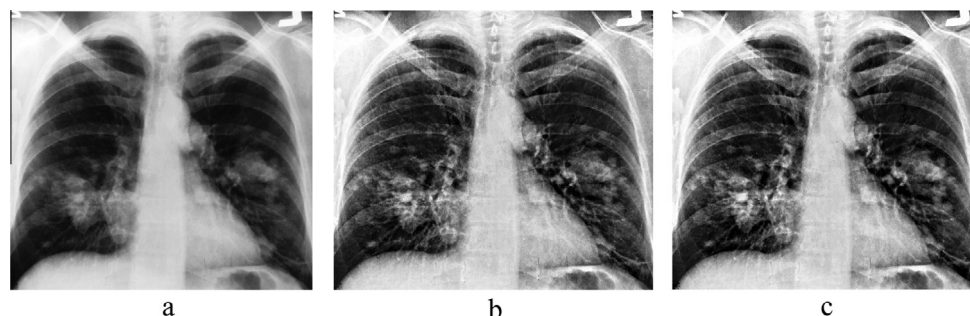


Fig. 6 (a) The original image, (b) the final enhanced image with the disk in size 30 and $CIR = 1$, (c) the enhanced image with the disk in size 40 and $CIR = 0.8533$, since image (e) has less values than the previous image, it is selected as the final image.

comparing the previous and the current enhanced images. This procedure continues while the returned values from CIR have been in an increasing manner. When CIR returns a smaller value, the procedure ends and the size of the previous mask is selected as the proper one to enhance the contrast of the image. It is CIR that compares the images resulted from two consecutive stages. If the value of the present comparison is larger than the previous one, the process continues. On the other hand, if CIR returns a smaller value, this means that the contrast of the new enhanced image is less than that of the previous image. Therefore, the image of the previous step is selected as the best enhanced image.

The change in the values of i and m continues up to the point when the returned image by CIR has a larger value than the previous image. When an image with a smaller CIR is created, the changing process stops and the image obtained from the penultimate step is elected as the final enhanced image. The penultimate values of i and m are the optimized values creating the desired image.

It should be noticed that the selection of proper initial values for i and m in Eq. (14) is dependent on the input image which is obtained through trial and error. An initial value of 30 for i presents desired response on most images. Figs. 4–6 show the results of the application of Eq. (14) and the selected optimized image by CIR. In the repetition process, the value of m in Figs. 4 and 5 is equal to 1 and 1.2 respectively. The initial value of i is 30 in both figures.

5. Results

As stated in Section 2, there are medical images with poor contrast which are difficult or impossible to study and acquire information from. So we should look for new methods to enhance the quality of such images.

Our proposed method which is based on mathematical morphology enhances the contrast of images and repairs their damaged parts. In fact, a Top-Hat transformation along with a disk structural element extracts white features such as blood vessels and aneurism (20). As explained in (21), it is difficult to use Top-Hat transforms in the images whose contrast changes much. Therefore, our proposed method can only be used to enhance medical images.

The reconstructed images of chest show a better resolution in lung tissue, especially the images whose initial quality is not appropriate; for example, see Fig. 7(a) that probably is taken in sleep mode. In the final image (Fig. 7(e)), small tumors have

become clearer, especially those that are superimposed on the ribs and are different from the main tissue. Two samples of these tumors which are circled in Fig. 7(e) show cancer progress more clearly.

In Fig. 7(b), the patient's left lung is hemorrhaging causing some of its tissue to be difficult to see. In emergency situations like this, catheters² are used. After inserting the catheters, Radiology images play an important role in locating the end of catheters and evaluating the possible side effects during its insertion. The enhanced image in Fig. 7(f) shows the left lung parenchyma and the end of catheters more clearly. Fig. 7(c) shows abdominal radiograph of an obese person which looks clearer in the reconstructed image shown in Fig. 7(g). Fig. 7(d) shows a foot radiograph. In Fig. 7(h), it is enhanced at the expense of fading the soft issue around the bone. Bigger vessels look sharper in the enhanced image of figure (m) while smaller vessels are invisible and more likely to be pathological. The kidney image after enhancing is shown in Fig. 7(n) that can be used instead of the original image in a segmentation process (22,23). The kidney in the enhanced image is more obvious, hence segmenting the image would be easier and more accurate compared to the one in the original image. In Fig. 7(o), the arrow implies a tumor as a prostate cancer. As seen, the diagnosis of tumor is easier than the original image in Fig. 7(k). Also, it can be used as an enhancement image in diagnosis methods of prostate cancer (24). Blood vessels can also be enhanced and then used for segmentation of 3D magnetic resonance angiography (25,26). The improved image of blood vessels can be seen in Fig. 7(p). We enhanced the contrast of heart images in Fig. 7(r). These can be used for the analysis of myocardial first-pass perfusion MR images (27).

The final result of the proposed method is compared with the method presented in (9) in terms of histogram equalization and contrast-limited adaptive histogram equalization (see Fig. 8). As it is clear in the images, the proposed method better enhances the contrast of the image and the details of the image are shown more accurately.

Since our proposed method goes through an exfoliation procedure, it is apparently superior to the Gamma method in enhancing the contrast and quality of the images to increase the accuracy of the diagnostic process. In contrast with the Gamma method, in this method, the resolution of the image is extremely high and the image details are better manifested.

² Catheters are thin tubes extruded from medical grade materials that can be inserted in the body to treat diseases or perform a surgical procedure.

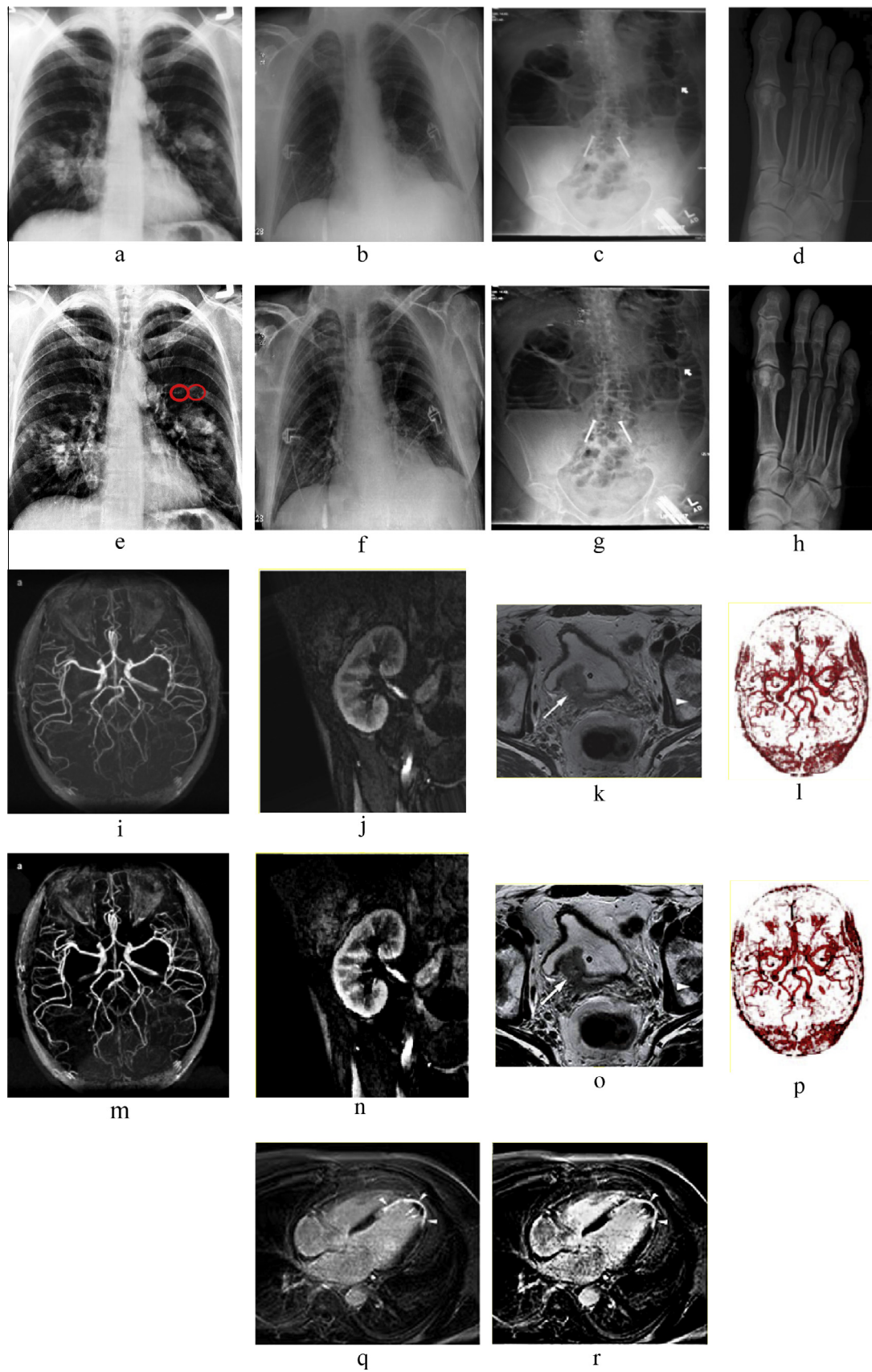


Fig. 7 The results from the proposed method. (a, b, c, d, i, j, k, l, and q) The original image, (e, f, g, h, m, n, o, p, and r) the enhanced image. The parameters are $m = 1.2$ and $i = 2$ and the disks in sizes 30, 40 and 50 are used according to each image.

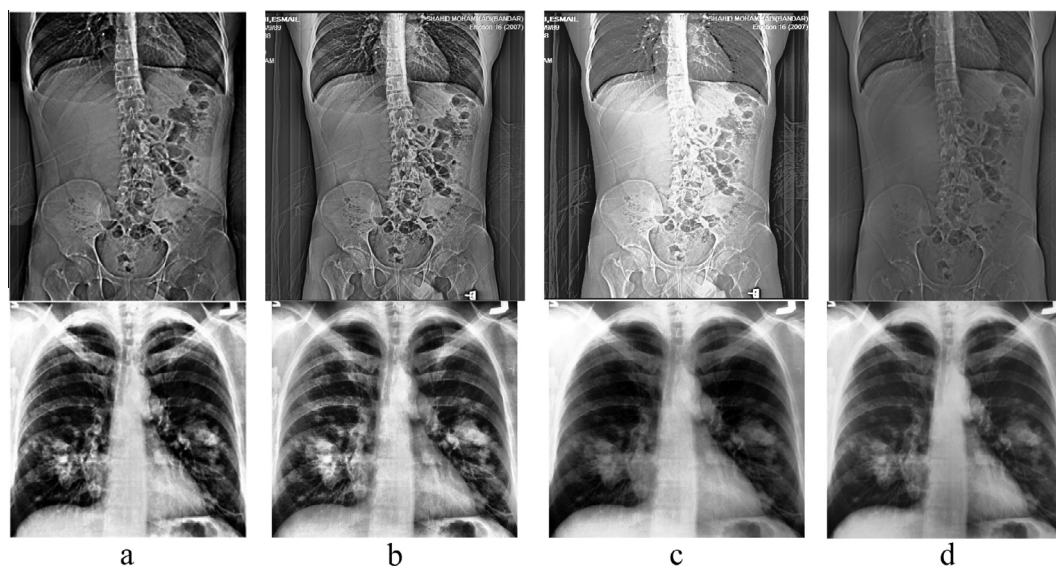


Fig. 8 (a) The results of applying the proposed method, (b) the results of applying CLAHE, (c) the results of applying histogram equalization, (d) the results of applying Gamma correction. (The original images are shown in Figs. 3 and 6.)

In contrast with other methods, morphological methods have very simple mathematical basics and acceptable computation time.

6. Conclusions

In this paper, a method using morphological Top-Hat transforms is presented to enhance the quality and contrast of medical images. In addition to its simplicity, this method has a high potentiality to process poor-quality medical image. The enhancement is obtained via an iterative exfoliation process evaluated using contrast improvement ratio measure. This approach can specify arbitrary organs overlapped in medical images for a better diagnosis. The comparison of histogram equalization and contrast-limited adaptive histogram equalization yielded from our proposed method and the one adopted from other existing medical image enhancement method indicates the superiority of the proposed method in improving the quality of medical images.

Conflict of interest

The authors declare that there are no conflicts of interest.

References

- (1) Yang Y, Su Z, Sun L. Medical image enhancement algorithm based on wavelet transform. *IEEE Electron Lett* 2010;46(2).
- (2) Sugimoto N, Imamura H, Sekiguchi H, Eiho S. Medical image processing in collaboration with medical researchers-imaging and image processing of cardiovascular disease dynamic images. In: Second international conference on informatics research for development of knowledge society infrastructure (ICKS); 2007. p. 77–86.
- (3) Vaida MF, Todica V. Dynamic adaptability of image processing components in medical applications. In: International symposium on signals, circuits and systems (ISSCS); 2007. p. 1–4.
- (4) Wang L, Jiang N, Ning X. Research on medical image enhancement algorithm based on GSM model for wavelet coefficients. *Phys Procedia* 2012;33:1298–303.
- (5) Cj M. Medical image processing: the characterization of display changes using histogram entropy. *Image Vis Comput* 1986;4: 197–202.
- (6) Qian W, Liya C, Dinggang S. Fast histogram equalization for medical image enhancement. In: 30th Annual international conference of the IEEE engineering in medicine and biology society; 2008. p. 2217–20.
- (7) Sengeer N, Bazarragchaa B, Tae Yun K, Heung Kook C. Weight clustering histogram equalization for medical image enhancement. In: IEEE international conference on communications workshops; 2009. p. 1–5.
- (8) Fu JC, Lien HC, Wong STC. Wavelet based histogram equalization enhancement of gastric sonogram images. *Comput Med Imaging Graph* 2000;24(2):59–68.
- (9) Asadi Amiri S, hassanpour H. A preprocessing approach for image analysis using gamma correction. *Int J Comput Appl* 2012;38:38–46.
- (10) Mahmoud TA, Marshall S. Medical image enhancement using threshold decomposition driven adaptive morphological filter. In: 16th European signal processing conference; 2008.
- (11) Chen T, Wu QH, Rahmani-Torkaman R, Hughes J. A pseudo top-hat mathematical morphological approach to edge detection in dark regions. *Pattern Recognit* 2002;35:199–210.
- (12) Sun KQ, Sang N. Morphological enhancement of vascular angiogram with multiscale detected by Gabor filters. *Electron Lett* 2008;44(2).
- (13) Wang X, Li M, Tang H. A modified homomorphism filtering algorithm for cloud removal. In: 3rd International congress on image and signal processing; 2010.
- (14) Serra J. *Image analysis and mathematical morphology*. Academic Press; 1983.
- (15) Xiangzhi B, Fugen Z. Multi structuring element top-hat transform to detect linear features. In: 10th International conference on signal processing; 2010. p. 877–80.
- (16) Jackway PT. Improved morphological top-hat. *Electron Lett* 2000;36:1194–5.
- (17) Bai X, Zhou F, Xue B. Image enhancement using multi scale image features extracted by top-hat transform. *Opt Laser Technol* 2012;44:328–36.

- (18) Kimori Y. Morphological image processing for quantitative shape analysis of biomedical structures: effective contrast enhancement. *J Synchrotron Radiat* 2013;848–53.
- (19) Ehsani SP, Mousavi HS, Khalaj BH. Chromosome image contrast enhancement using adaptive, iterative histogram matching. In: *Machine vision and image processing (MVIP)*; 2011.
- (20) Meyer F. Iterative image transforms for the automatic screening of cervical smears. *J Histochem Cytochem* 1979;27:128–35.
- (21) Vincent L, Masters B. Morphological image processing and network analysis of corneal endothelial cell images. *Image Algebra Morphol Image Process III* 1992;1769:212–26.
- (22) Khalifa F et al. Dynamic contrast-enhanced MRI-based early detection of acute renal transplant rejection. *IEEE Trans Med Imaging* 2013;32(10):1910–27.
- (23) Khalifa F et al. A comprehensive non-invasive framework for automated evaluation of acute renal transplant rejection using DCE-MRI. *NMR Biomed* 2013;26(11):1460–70.
- (24) Firjani A et al. A diffusion-weighted imaging based diagnostic system for early detection of prostate cancer. *J Biomed Sci Eng* 2013;6(3):346–56.
- (25) El-Baz A et al. Precise segmentation of 3D magnetic resonance angiography. *IEEE Trans Biomed Eng* 2012;59(7):2019–29.
- (26) El-Baz A et al. Fast accurate unsupervised segmentation of 3d magnetic resonance angiography. In: Suri J, Kathuria C, Molinari F, editors. *Handbook of atherosclerosis disease management*. Springer; 2011. p. 411–29, ISBN: 978-1-4419-7221-7 [chapter 14].
- (27) Beache GM et al. Fully automated framework for the analysis of myocardial first-pass perfusion MR images. *Med Phys* 2014;41(10).